Heterogeneous relaxation patterns in supercooled liquids studied by solvation dynamics

Hauke Wendt
Max-Planck-Institut für Polymerforschung, Ackermannweg 10, 55128 Mainz, Germany

Ranko Richert
Department of Chemistry and Biochemistry, Arizona State University, Tempe, Arizona 85287-1604

(Received 17 September 1999)

We have measured the solvation dynamics of a dipolar supercooled liquid near its glass transition in a temperature range in which the average structural relaxation time varies more than four orders of magnitude. The analysis of the time dependent average emission energy and the inhomogeneous linewidth of the $S_0 \leftarrow T_1(0\text{-}0)$ transition reveals that the orientation correlation decay pattern intrinsic in each relaxing unit is associated with a stretching exponent $\beta_{\rm intr}=1.00\pm0.08$ in the entire range $T_g \leqslant T \leqslant T_g+6$ K. Our analysis also allows one to detect fluctuations in terms of the resulting apparent homogeneity within the long time tail of the decay. Even at times significantly exceeding the average structural relaxation time, no sign of a transition towards purely exponential or otherwise homogeneous behavior could be observed. This implies that even at $t \approx 50\langle\tau\rangle_{\rm KWW}$ the individual time constants remain correlated to their initial values at $t=0$.

PACS number(s): 64.70.Pf, 78.47.+p, 77.22.Gm, 05.40.−a

I. INTRODUCTION

A characteristic feature of supercooled liquids and other disordered materials is their nonexponential behavior as regards the relaxation dynamics [1]. In recent years, heterogeneities with respect to the relaxation time have been recognized as the source of these complex correlation functions [2–7]. The majority of experimental techniques measure the ensemble averaged two time correlation function only. Therefore, they are not sensitive to a spatial variation of the characteristic relaxation times. Other approaches, like NMR [2,8,9], photobleaching experiments [4,10], or dielectric hole-burning techniques [5,11,12] can exploit spectral selectivity in order to reveal the heterogeneous nature. These methods allow for probing a subensemble whose response differs initially from that of the average but becomes indistinguishable from the average after some evolution period [4,10,13]. Therefore, heterogeneity with respect to molecular dynamics is not a static property. Instead, several experimental results suggest that fluctuations of the local relaxation times tend to restore ergodicity on the time scale of the structural relaxation.

A different approach to the details of molecular dynamics is by measuring higher moments of the two-time correlation function [6,7,14,15]. It has been demonstrated previously that solvation dynamics experiments on highly supercooled liquids yield not only the mean $\phi(t)$ but also the variance $\rho(t)$ of the relaxing quantity [6]. In order to clarify the meaning of $\rho(t)$, the ensemble averaged relaxation function $\phi(t)$ is written as the mean of local contributions $\chi(t,\tau)$ with respect to the probability density $g(\tau)$ of finding a particular value of τ,

$$\phi(t)=\int_0^\infty g(\tau)\chi(t,\tau)d\tau=\langle\chi(t,\tau)\rangle. \quad (1)$$

The brackets $\langle\,\rangle$ represent ensemble averages throughout the paper. In the homogeneous case, no variation of $\chi(t,\tau)$ exists, i.e., $g(\tau)=\delta(\tau-\tau_0)$ and $\chi(t,\tau)=\phi(t)$. Consequently, the variance $\rho(t)=\langle\chi^2(t,\tau)\rangle-\langle\chi(t,\tau)\rangle^2$ remains zero for all times in this situation. Heterogeneity is present whenever $g(\tau)$ has a finite width and $\chi(t,\tau)$ is accordingly more exponential than is $\phi(t)$. The degree of exponentiality as regards the intrinsic relaxation pattern can be cast into a single parameter, $\beta_{\rm intr}$, by chosing the stretched exponential form, $\chi(t,\tau)=\exp[-(t/\tau)^{\beta_{\rm intr}}]$ [14]. In this case, $\rho(t)$ takes the form

$$\rho(t)=\langle\chi^2(t,\tau)\rangle-\langle\chi(t,\tau)\rangle^2=\phi(2^{1/\beta_{\rm intr}}t)-\phi^2(t). \quad (2)$$

In contrast to the mean, $\phi(t)$, the concomitant second central moment $\rho(t)$ is seen to depend explicitly on $\beta_{\rm intr}$. Examples of $\rho(t)$ for various values of $\beta_{\rm intr}$ are given in Fig. 1. In recent papers, the inhomogeneous linewidths taken from solvation dynamics experiments have been analyzed in terms of $\rho(t)$. Based on the simplified model of a static distribution of τ, it was shown that $\beta_{\rm intr}\geqslant 0.8$ at $T=T_g+3$ K for the glass-forming liquid 2-methyltetrahydrofuran [15].

The aim of the present paper is to assess the local relaxation patterns on the basis of substantially improved solvation dynamics data relative to the previous work [6]. The present experiments cover a temperature range in which the structural relaxation time varies more than four orders of magnitude. For the correlation decay pattern intrinsic in each relaxing unit we find a stretching exponent $\beta_{\rm intr}=1.00\pm0.08$ in the entire range $T_g=91\,{\rm K}\leqslant T\leqslant 97\,{\rm K}$, without having to invoke a particular relaxation model.

II. EXPERIMENTS

The glass-forming ($T_g=91$ K) solvent 2-methyltetrahydrofuran (MTHE) is obtained from Aldrich and freshly distilled. The phosphorescent chromophore quinoxaline (QX) has been purified by sublimation. MTHF is then doped with QX at a concentration level of 10^{-4} mole/mole and immediately filled into a clean brass cell with a sapphire window

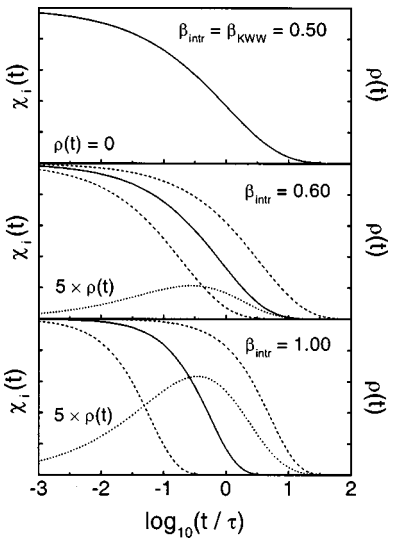

FIG. 1. Individual relaxation patterns $\chi_i(t)$ for a common ensemble averaged decay $\phi(t)=\langle\chi_i(t)\rangle$ of the KWW type with $\tau_{\mathrm{KWW}}=1$ and $\beta_{\mathrm{KWW}}=0.5$ and for various values of $\beta_{\mathrm{intr}}=0.50$, 0.60, and 1.00. The decays $\chi_i(t)$ in each panel are traces of exp $[-(t/\tau_i)^{\beta_{\mathrm{intr}}}]$ with $\ln(\tau_i)=\langle\ln(\tau_i)\rangle\pm$ the standard deviation of $\ln(\tau_i)$. The dotted $\rho(t)=\langle\chi_i(t)^2\rangle-\langle\chi_i(t)\rangle^2$ curves represent the variances of the site specific decays.

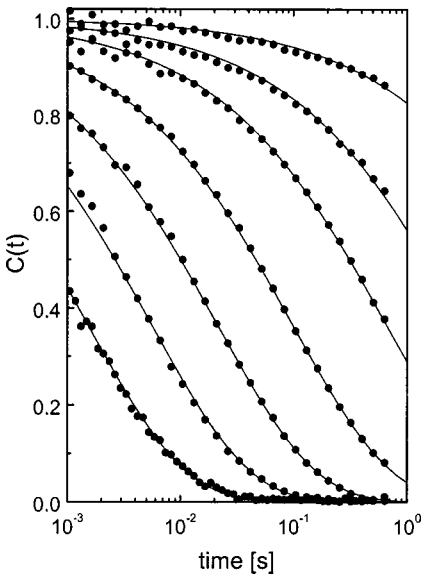

FIG. 2. Normalized Stokes shift results $C(t)$ (symbols) for the system QX/MTHF at various temperatures from $T=91$ K to 97 K in steps of 1 K, in the order of the slowest to fastest decay. The solid lines are fits to the $C(t)$ data using a stretched exponential $\phi(t)$ $=\exp[-(t/\tau_{\mathrm{KWW}})^{0.5}]$.

which is vacuum sealed by a Kalrez o-ring. The cell is mounted to the cold stage of a closed cycle He refrigerator (Leybold, RDK 10-320, RW 2) and temperature stability within ± 30 mK was achieved by a temperature controller (Lake Shore, LS 330) equipped with calibrated diode sensors. Samples are allowed to equilibrate for a sufficiently long time in the highly viscous regime.

An excimer laser (Radiant Dyes, RD-EXC-100) operated at $\lambda_{\mathrm{ex}}=308$ nm with a repetition rate of 1 Hz and attenuated to irradiate the sample at ≈ 10 mJ per pulse served for exciting the dye electronically. The phosphorescence emission is coupled via fibre optics to a monochromator (EG&G, 1235) and registered by a MCP intensified diode array camera (EG&G, 1455B-700-HQ) with controller (EG&G, 1471A), gating options (EG&G, 1304), and synchronization facilities (SRS, DG-535). The spectra consist of 730 channels with a resolution of 0.04 nm/channel and were wavelength calibrated with Xe and Kr calibration lamps. The time resolution is defined by gating the camera with variable gate delays t_d and gate widths $t_w \leqslant 10$ ms. We refrained from invoking the cw mode of the camera for delay times exceeding 20 ms because the cw mode leads to systematic errors regarding both spectral shape and time scale assignment. For the present experiments the delays were scanned logarithmically within the range $100\,\mu\mathrm{s} \leqslant t_d \leqslant 1$ s, with the widths set to $t_w = 0.1 t_d$ for $t_d \leqslant 100$ ms and $t_w = 10$ ms otherwise. Every final spectrum is obtained by averaging over the signals from 1200 excitation pulses.

III. RESULTS

The $S_0 \leftarrow T_1(0\text{-}0)$ phosphorescence spectra of QX in MTHF have been recorded as a function of time and temperature. For the emission line shapes we observe Gaussian profiles, i.e., the intensity $I(\nu)$ follows

$$I(\nu)=\frac{1}{\sigma\sqrt{2\pi}}\exp\left[-\frac{(\nu-\langle\nu\rangle)^2}{2\sigma^2}\right]. \tag{3}$$

Therefore, the $S_0 \leftarrow T_1(0\text{-}0)$ transition is entirely characterized by two quantities, the average energy $\langle\nu(t,T)\rangle$ and the Gaussian width $\sigma(t,T)$, both being a function of time and temperature. The limiting values $\langle\nu(t\rightarrow 0)\rangle$ and $\langle\nu(t\rightarrow\infty)\rangle$ are well defined and serve for constructing the so-called ''Stokes shift correlation function''

$$C(t)=\frac{\langle\nu(t)\rangle-\langle\nu(\infty)\rangle}{\langle\nu(0)\rangle-\langle\nu(\infty)\rangle}, \tag{4}$$

which is the appropriate quantity for focusing on the dynamical aspects of the solvation process, while disregarding the absolute energy scale. We also define the total Stokes shift $\Delta\nu=\langle\nu(t=0)\rangle-\langle\nu(t=\infty)\rangle$ and the steady state linewidth $\sigma_0=\sigma(t=\infty)=\sigma(t=0)$.

The $C(t)$ results for temperatures $91\,\mathrm{K} \leqslant T \leqslant 97\,\mathrm{K}$ are plotted in Fig. 2. In the present temperature range the average structural relaxation times vary by a factor of 2×10^4, from 1.5×10^{-3} s to 27 s. The $C(t)$ curves are well represented by stretched exponential decays with a temperature invariant exponent $\beta_{\mathrm{KWW}}=0.5$. This applicability of time-temperature superposition allows to cast the data sets into the master plot, $C(t)$ versus t/τ_{KWW}, in Fig. 3. The inset of Fig. 3 displays the $\tau_{\mathrm{KWW}}(T)$ data used for this rescaling. The $\sigma(t,T)$ data are compiled in Fig. 4, again after reducing the time scales to t/τ_{KWW}. For reasons which will be explained below, the linewidth results are plotted as $[\sigma^2(t)-\sigma_0^2]/\Delta\nu^2$.

IV. DISCUSSION

Solvation dynamics associated with dipolar systems is governed by the orientational aspects of molecular dynamics

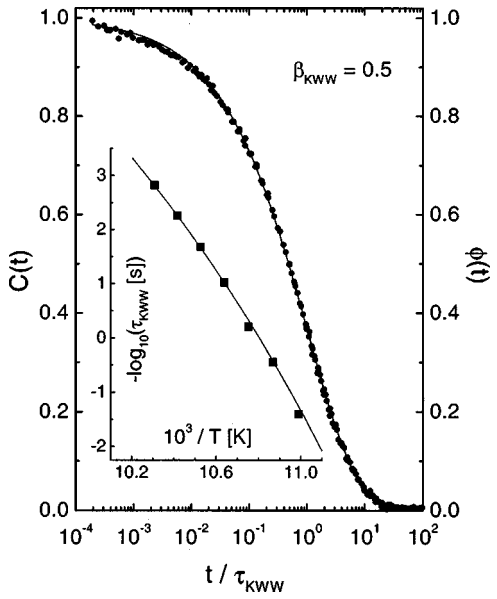

FIG. 3. Master plot $C(t)$ (symbols) versus t/τ_{KWW} based on the data of Fig. 2. The solid line is a fit using a stretched exponential $\phi(t)=\exp[-(t/\tau_{\mathrm{KWW}})^{0.5}]$. The inset shows an Arrhenius plot of $\tau(T)$ based on the fits of Fig. 2.

[16,17]. Because the first solvent shell around a probe molecule is dominant regarding the electrostatical solute-solvent interactions, the time dependent free energies of solvation can be considered analogous to the local dielectric relaxation [18,19]. However, the solvation experiments yield not only the average energies, but also the entire spatial distribution in terms of the inhomogeneously broadened emission profile. That the width σ of these spectra is time dependent has been recognized already in earlier solvation dynamics experiments [20,21]. Within the framework of solvation theories, no prediction for such time dependence of the linewidth has been advanced, because the dynamical behavior of each dipole is identically modeled by the macroscopic dielectric function $\epsilon^*(\omega)$. In what follows, the alternative picture of spatially varying relaxation times is addressed in quantitative detail.

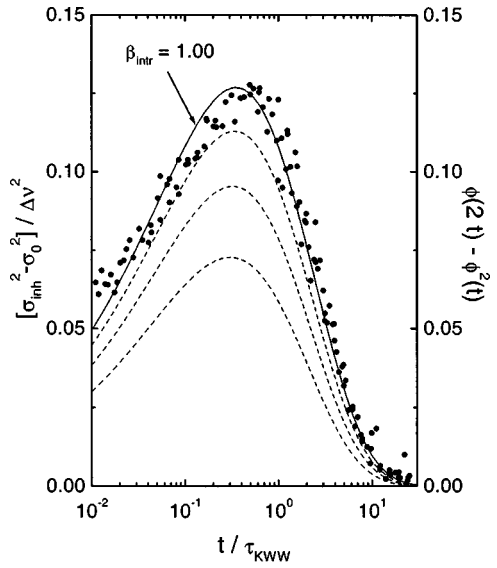

FIG. 4. Master plot $\rho(t)$ (symbols) versus t/τ_{KWW} based on the $\sigma_{\mathrm{intr}}(t)$ data of the system QX/MTHF at temperatures $91\,\mathrm{K}\leqslant T\leqslant 97\,\mathrm{K}$. The lines are predicted $\rho(t)$ curves using $\phi(t)=\exp[-(t/\tau_{\mathrm{KWW}})^{0.5}]$ for various values of $\beta_{\mathrm{intr}}=1.0$, 0.9, 0.8, and 0.7, in the order from top to bottom curve. The case $\beta_{\mathrm{intr}}=\beta_{\mathrm{KWW}}=0.5$ leads to $\rho(t)\equiv 0$.

For rationalizing $\sigma(t)$ in the course of a solvation process, both site specific quantities, the solvation free energy ν and the characteristic time scale τ, need to be considered. For a particular site, the energetic relaxation, $\nu(t)$, can be written as [6]

$$\nu(t)=\nu(\infty)+\Delta\nu\,\chi(t,\tau), \tag{5a}$$

$$\nu(t)=\nu(\infty)+\Delta\nu\,\exp[-(t/\tau)^{\beta_{\mathrm{intr}}}]. \tag{5b}$$

Since both quantities $\nu(\infty)$ and $\chi(t,\tau)$ are independent random variables, the mean $\langle\nu(t)\rangle$ and the variance $\sigma^2(t)$ of $\nu(t)$ can be obtained by adding the individual corresponding moments [15]. This establishes the following correlation between $\sigma(t)$ and $C(t)=\phi(t)$:

$$\frac{\sigma^2(t)-\sigma_0^2}{\Delta\nu^2}=\rho(t)=\langle\chi^2(t,\tau)\rangle-\langle\chi(t,\tau)\rangle^2, \tag{6a}$$

$$\frac{\sigma^2(t)-\sigma_0^2}{\Delta\nu^2}=C(2^{1/\beta_{\mathrm{intr}}}t)-C^2(t). \tag{6b}$$

The quantities $\sigma(t)$, σ_0, $\Delta\nu$, and $C(t)$ are well defined by experiment. The above cases Eq. (5a) and Eq. (6a) are of general validity, whereas setting $\chi(t,\tau)=\exp[-(t/\tau)^{\beta_{\mathrm{intr}}}]$ in Eq. (5b) and Eq. (6b) assumes the absence of fluctuations regarding τ. The only unknown parameter in Eq. (6b) is β_{intr}, which quantifies the degree of nonexponentiality intrinsic in each local relaxing unit. Therefore, this equation provides a straightforward link between the normalized Stokes shift response function, $C(t)$, and the concomitant linewidth, $\sigma(t)$, which through β_{intr} depends on $g(\tau)$. It predicts that an excess linewidth, $\sigma(t)>\sigma_0$, appears in the course of a solvation process if (and only if) the underlying dynamical processes exhibit a spatial variation of time scales [15]. Conversely, one could conclude on entirely homogeneous dynamics from an observation of a time invariant linewidth, $\sigma(t)\equiv\sigma_0$.

In order to analyze the present solvation data along Eq. (6b), it is convenient to have a simple analytical function which matches the $C(t)$ data, such that $C(2^{1/\beta_{\mathrm{intr}}}t)$ can be obtained easily. Both Fig. 2 and Fig. 3 demonstrate that a stretched exponential or Kohlrausch-Williams-Watts (KWW) decay,

$$\phi_{\mathrm{KWW}}(t)=\exp[-(t/\tau_{\mathrm{KWW}})^{\beta_{\mathrm{KWW}}}], \tag{7}$$

with $\beta_{\mathrm{KWW}}=0.5$ is appropriate for handling $C(t)$ at arbitrary times. Furthermore, the observation of a temperature invariant β_{KWW} makes it sufficient to analyze the $\sigma(t)-C(t)$ relation on the basis of the master curves, where the variable t/τ_{KWW} is used instead of the absolute time. Figure 4 compares the experimental results $[\sigma^2(t)-\sigma_0^2]/\Delta\nu^2$ with the predictions, $C(2^{1/\beta_{\mathrm{intr}}}t)-C^2(t)$, for various values of β_{intr} using $C(t)=\phi_{\mathrm{KWW}}(t)$. In this plot the solid line refers to $\beta_{\mathrm{intr}}=1$, where $\rho(t)=C(2t)-C^2(t)$. This case corresponds

to intrinsic relaxation patterns which are purely exponential and results in an excellent agreement with the experimental findings. The dashed curves in Fig. 4 are for $\beta_{\rm intr}=0.9$, 0.8, and 0.7, where already $\beta_{\rm intr}=0.9$ is an inferior fit relative to $\beta_{\rm intr}=1$.

An unbiased approach for assessing the intrinsic relaxation pattern is a statistical analysis of the experimental data according to

$$\beta_{\rm intr}=\beta_{\rm KWW}\frac{\ln 2}{\ln\left[\frac{\ln(\rho(t)+\phi^2(t))}{\ln(\phi(t))}\right]}, \tag{8}$$

where $\beta_{\rm intr}$ is now expressed in terms of experimentally well defined quantities, $\beta_{\rm KWW}$, $\rho(t)=[\sigma^2(t)-\sigma_0^2]/\Delta v^2$, and $\phi(t)=C(t)$. The mean and standard deviation for $\beta_{\rm intr}$ have been computed in the range $2\times10^{-2}\leqslant t/\tau_{\rm KWW}\leqslant 2$ yielding $\beta_{\rm intr}=1.001\pm0.077$. This result states unambiguously that the orientational correlation decays exponentially as far as the local response around a probe molecule is concerned. Within the present experimental range, $91\,{\rm K}\leqslant T\leqslant 97\,{\rm K}$ or $T_g\leqslant T\leqslant T_g+6$ K or $3\times10^{-3}\,{\rm s}\leqslant\langle\tau\rangle\leqslant 54\,{\rm s}$, no indication towards a systematic deviation from $\beta_{\rm intr}=1$ can be found. It shall be noted that an analogous treatment with basic functions $\chi(t,\tau)$ other than the stretched exponential is possible.

A number of previous investigations can be found which have quantified the degree of heterogeneity measured either by η or by $\beta_{\rm intr}$. Regarding materials of low molecular weight, these studies include propylene carbonate investigated by nonresonant dielectric hole burning at $T=T_g+4$ K ($\tau=100$ ms, $\beta_{\rm KWW}=0.72$) and *o*-terphenyl (OTP) using multidimensional NMR techniques at $T=T_g+11$ K ($\tau=16$ ms, $\beta_{\rm KWW}=0.42$) [7]. In these two cases, the experimental observations are compatible with the purely heterogeneous case, $\beta_{\rm intr}=1$. NMR techniques have also been applied to polymeric systems, polystyrene (PS) at $T=T_g+13$ K ($\tau=6.5$ ms, $\beta_{\rm KWW}=0.45$) and polyvinylacetate (PVAc) at $T=T_g+10$ K ($\tau=20$ ms, $\beta_{\rm KWW}=0.52$) [22]. The result for these polymers is that their intrinsic relaxation is associated with back-jump probabilities $R\approx0.3\pm0.1$ for PS and $R\approx0.4\pm0.05$ for PVAc. $R>0$ states that the intrinsic segmental relaxation is not entirely exponential. Based on the empirical relation $\beta_{\rm intr}\approx1-R/2$, valid for $0\leqslant R\leqslant 0.6$, the values of R translate into $\beta_{\rm intr}\approx0.85$ ($\eta=0.73$) for PS and $\beta_{\rm intr}\approx0.80$ ($\eta=0.58$) for PVAc. It appears that glass-forming materials of low molecular weight are associated with pure heterogeneity, $\beta_{\rm intr}=1$, while polymeric systems are subject to homogeneous contributions as regards their segmental dynamics. The drawback of the methods compiled above is that $\beta_{\rm intr}$ is evaluated at a single temperature per material only and that the overall range of relaxation times remained rather limited, $6.5\,{\rm ms}\leqslant\tau\leqslant 100\,{\rm ms}$.

Let us now turn to the role of the fluctuations or rate exchange regarding local relaxation time constants. As required by ergodicity, these fluctuations let a time constant τ associated with a particular site visit the entire relevant τ-space in the long time limit. There is evidence that the time scale, τ_x, of these rate exchanges matches that of the structural relaxation, τ_α [3], with a tendency towards longer lived heterogeneities reported for *o*-terphenyl as the temperature is lowered near T_g [10]. The relation $\tau_x\geqslant\tau_\alpha$ is generally accepted.

Independent of their time scale, fluctuations have not been incorporated explicitly into the distribution of site specific relaxation times, quantified in Eq. (1) by $g(\tau)$. However, the only demand regarding $g(\tau)$ is that the correlation decay $\phi(t)$ can be cast into the form of Eq. (1) in which $g(\tau)$ has the properties of a probability density function. This constitutes no practical restriction because any physically sensible relaxation pattern can be translated into an appropriate distribution of τ. In the case of fluctuations, the probability density $g(\tau)$ in Eq. (1) refers to some ''effective'' quantity [23], but the validity of Eq. (6a) remains unaffected, which states that the linewidth $\sigma(t)$ is proportional to the variance of $\chi(t,\tau)$. Our evaluation regarding $\beta_{\rm intr}$ does assume the absence of fluctuations, but in view of $\tau_x\geqslant\tau_\alpha$ they remain insignificant in the time regime $t<2\tau_{\rm KWW}$ in which the peak of $\rho(t)$ is positioned. In any case is the prediction based on static heterogeneity entirely consistent with our observations in Fig. 4. The bottom line of these arguments is that the above statement, $\beta_{\rm intr}=1$, holds irrespective of the persistence time of site specific dynamics. In terms of the heterogeneity scale η defined previously [7],

$$\eta=\frac{\beta_{\rm intr}-\beta_{\rm KWW}}{1-\beta_{\rm KWW}}, \tag{9}$$

the present results are consistent with a degree of heterogeneity at the theoretical maximum, $\eta=1$.

An obvious consequence of fluctuations or rate exchange is that they give rise to purely exponential ensemble averaged decays at times $t\gg\tau_x$. This is equivalent to apparent homogeneity for times exceeding those required for all sites to sample the entire τ-space. Unless $\tau_x\gg\tau_\alpha$, $g(\tau)$ should be understood as an effective probability density. Its profile results from both, the ''true'' underlying static density $g_s(\tau)$ and the effect of rate exchange, which leads to $g(\tau)$ being narrower than $g_s(\tau)$. The case of slow fluctuations would result in $g(\tau)\approx g_s(\tau)$. The present observation of a temperature invariant $\beta_{\rm KWW}$ implies a $g(\tau)$ whose shape is temperature independent. This feature of MTHF in its viscous liquid regime suggests either that the ratio Q of the fluctuation or rate exchange time to the structural relaxation time, $Q=\langle\tau_x\rangle/\langle\tau_\alpha\rangle$ [24], is also temperature independent or that $\langle\tau_x\rangle\gg\langle\tau_\alpha\rangle$ in this temperature regime.

In principle, there exists a further scenario which is compatible with $\rho(t)$ exhibiting a maximum as found for the present data. It is the possibility that the short time dynamics are heterogeneous, while true or apparent homogeneity prevails at longer times. Such a transition from an exponential to a highly nonexponential character regarding the intrinsic relaxation pattern can in principle be thought of by invoking memory terms [22] which gain importance as time proceeds. Compared to the effects of fluctuations, such a picture also gives rise to homogeneous behavior at longer times, but without necessarily leading to an exponential overall decay $\phi(t)$. Because the short time dynamics are still assumed heterogeneous, the variance $\rho(t)$ of the random variable $\chi(t,\tau)$ would initially increase as observed. If t_m denotes the time after which the relaxation is homogeneous in the sense that

all intrinsic relaxations are equally tracking the ensemble averaged behavior, then for $t>t_m$ all individual relaxors will proceed with a common decay pattern $\chi(t,\tau)=\phi(t)$. In reality, such a transition would be a gradual rather than an abrupt change. Let $\phi_m(t)=\phi(t>t_m)$ and $\rho_m(t)=\rho(t>t_m)$ denote the mean and variance as above but for the time regime $t>t_m$. Assuming $\beta_{\rm intr}=1$ for times $t<t_m$ leads to

$$\phi_m(t)=\int_0^\infty g(\tau)\exp(-t_m/\tau)\frac{\phi(t)}{\phi(t_m)}d\tau=\phi(t),\quad t>t_m, \tag{10}$$

where only the amplitudes at time t_m depend on τ. In this equation, $g(\tau)\exp(-t_m/\tau)$ expresses the distribution of amplitudes at $t=t_m$ and $\phi(t_m)$ rescales the time dependent term to assume unity at $t=t_m$. The concomitant dynamics leading to $\phi_m(t)$ are now homogeneous but their ensemble average is maintained, i.e., $\phi_m(t)=\phi(t)$. For the variance $\rho_m(t)$ of the amplitudes $\chi(t,\tau)=\exp(-t_m/\tau)\phi(t)/\phi_m(t)$ we find

$$\rho_m(t)=\phi^2(t)\left[\frac{\phi(2t_m)}{\phi^2(t_m)}-1\right],\quad t>t_m. \tag{11}$$

The interesting feature of the above two quantities is that $\sigma_m(t)=\sqrt{\rho_m(t)}$ and $\phi_m(t)$ decay with the same functional form for the time dependence as soon as the dynamics appear to be homogeneous. In other words, the quantity

$$\frac{\sqrt{\rho_m(t)}}{\phi_m(t)}=\sqrt{\frac{\phi(2t_m)}{\phi^2(t_m)}-1}=\text{const},\quad t>t_m \tag{12}$$

will be time invariant in cases where the individual relaxation patterns cease to be site specific. Relative to the prediction $\rho(t)\equiv 0$ for a system whose dynamics are homogeneous at all times, this new condition expressed in Eq. (12) can be used as a more general indicator of homogeneity, applicable also to limited time ranges. On the basis of the present experimental data, the condition given by Eq. (12) is readily tested by plotting $\rho^{0.5}(t)/C(t)$ as a function of time. This is done in Fig. 5 using the master curves, i.e., by plotting $\rho^{0.5}(t)/C(t)$ versus $t/\tau_{\rm KWW}$. Since this quantity increases monotonically over the entire experimental range, we conclude that the dynamics are incompatible with any tendency towards homogeneity in the present experimental range. Similarly, Fig. 6 shows for $t_m/\tau_{\rm KWW}=1$, 2, and 4 that $\rho_m(t)$ decays steeper than does the experimental data, thereby supporting the above notion.

A system which is still heterogeneous for times $t\gg\tau_\alpha$ could also satisfy the condition $\sqrt{\rho_m(t)}/\phi_m(t)=\text{const}$, but only in terms of an exponential decay regarding the ensemble average. Accordingly, rate exchange mechanisms associated with a time scale τ_x give rise to apparent homogeneity at times $t\gg\tau_x$, and will lead to both, an exponential long time decay of $\phi(t)$ and a time invariant value of $\sqrt{\rho_m(t)}/\phi_m(t)$. The quantity $\sqrt{\rho_m(t)}/\phi_m(t)$ appears to be more decisive in this respect, because the data in Fig. 5 is clearly increasing with time in the regime $t>10\times\tau_{\rm KWW}$, in which a deviation of $C(t)$ from exponentiality is not at all obvious. Similarly, the prediction for homogeneous behavior at times exceeding $t_m=10\times\tau_{\rm KWW}$ (dashed lines in Fig. 5 and Fig. 6) deviates more clearly from the current data in the $\sqrt{\rho(t)}/C(t)$ plot in Fig. 5 than in the $\rho(t)$ plot in Fig. 6.

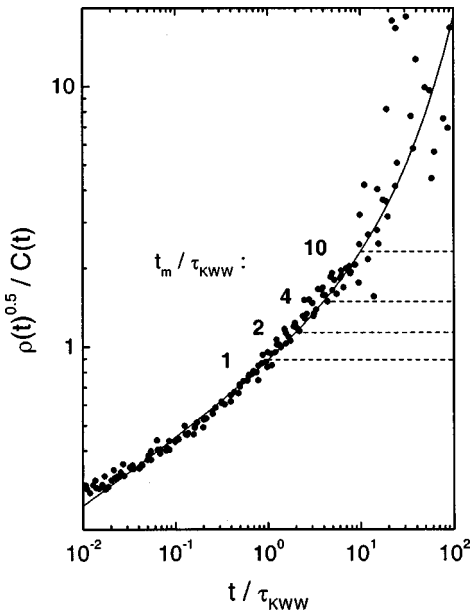

FIG. 5. Master plot of $\rho^{0.5}(t)/C(t)$ (symbols) versus $t/\tau_{\rm KWW}$ based on the solvation data of the system QX/MTHF at temperatures 91 K$\leqslant T\leqslant$97 K. The line is the prediction for the heterogeneous case with $\beta_{\rm intr}=1.0$. Homogeneity for $t>t_m$ would lead to the horizontal dashed curves drawn for the cases $t_m/\tau_{\rm KWW}=1$, 2, 4, and 10 as indicated.

The analysis of the present data along the lines of Eq. (12) as in Fig. 5 thus reveals that the local relaxation patterns remain site-specific even at times as long as $t=10^2\times\tau_{\rm KWW}=50\times\langle\tau\rangle_{\rm KWW}$. Note that the bulk of the data points in the range $t>\langle\tau\rangle_{\rm KWW}$ are associated with the higher temperatures, 95 K$\leqslant T\leqslant$97 K. We conclude that the fluctuations of site specific time constants τ are not efficient enough for

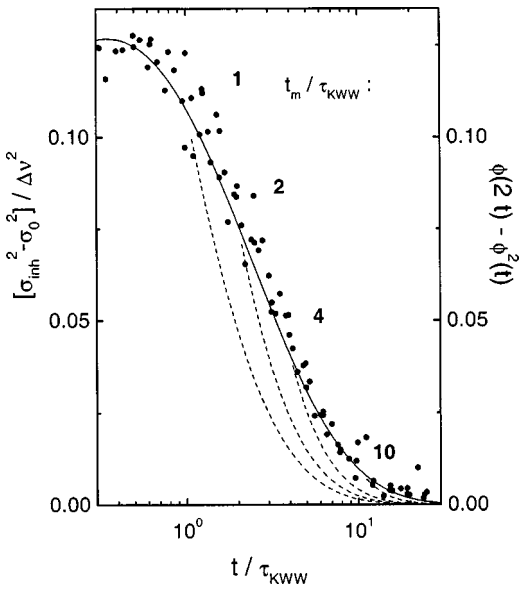

FIG. 6. Plot of $\rho(t)$ as in Fig. 4 but including the predictions $\rho_m(t)$ (dashed lines) for homogeneous behavior at times $t>t_m$. These curves represent the cases $t_m/\tau_{\rm KWW}=1$, 2, 4, and 10 as indicated.

allowing a site to visit the entire τ-space within a period of $50\times\langle\tau\rangle_{\mathrm{KWW}}$. This observation is compatible either with slow rate exchanges, $Q=\langle\tau_x\rangle/\langle\tau_\alpha\rangle\gg 1$, or with faster fluctuations, say $Q\approx 1$, if the time constant changes are confined to a limited range around the initial value of τ. We suspect that heterogeneously relaxing units subject to a simple correlation decay of the τ's with a time scale τ_x around $\langle\tau_\alpha\rangle \approx\langle\tau\rangle_{\mathrm{KWW}}$ should give rise to exponentiality regarding $\phi(t)$ at times $t\leqslant 50\times\langle\tau\rangle_{\mathrm{KWW}}$, because $\beta_{\mathrm{KWW}}=0.5$ relates to an overall τ-distribution of moderate width. The reliable statements regarding fluctuations which can be inferred from the present measurements are that there remains a non-vanishing correlation between $\tau(t\approx 50\times\langle\tau\rangle_{\mathrm{KWW}})$ and $\tau(t=0)$ at a given site and that the data are entirely consistent with the absence of rate-exchange. More quantitative estimates on a lower limit for Q on the basis of the present results require a model which specifies how a site samples the τ space as a function of time. However, such detailed informations about the mechanisms involved in these fluctuations are not available to date. The possibility that a wide spectrum of time scales is involved in these fluctuations can be regarded in terms of a stretched exponential exchange process [25]. In any case, it is insufficient to address a characteristic fluctuation time without specifying the associated displacement $\Delta\tau$ in τ space, quite in analogy to anomalous diffusion. It should further be considered that different experimental approaches to rate-exchange times are likely to probe different measures of $\Delta\tau$.

The first assessment of exchange times has been reported by Spiess and co-workers [2,8] for PVAc at a temperature $T=T_g+20\,\mathrm{K}$ using a reduced 4D-NMR method, which resulted in $Q=\langle\tau_x\rangle/\langle\tau_\alpha\rangle\approx 2$. For PS at $T=T_g+10\,\mathrm{K}$ Kuebler *et al.* [24] arrived at $Q=1$ on the basis of solid-state NMR echo techniques. Cicerone and Ediger [4,26] found $Q\approx 100$ for supercooled OTP at $T=T_g+1\,\mathrm{K}$ using the dynamically selective photobleaching method. For the same material but at a higher temperature, $T=T_g+10\,\mathrm{K}$, Böhmer *et al.* [13] reported $Q\approx 1$ based on multidimensional NMR measurements. More recently, Wang and Ediger [10] have shown that Q decays gradually from 540 to 2 in OTP as the temperature increases from T_g to $T_g+10\,\mathrm{K}$ Dynamical heterogeneities observed in nonresonant hole-burning (NHB) experiments on propylene carbonate and glycerol by Schiener *et al.* [5,11] are compatible with $Q=1$, whereas Kircher *et al.* [27] observed long lived ($Q\gg 1$) heterogeneities in a relaxor ferroelectric. Based on these observations, dynamical heterogeneities in supercooled liquids of low molecular weight appear to be longer lived only in the immediate vicinity of the glass transition temperature. The present observation of $Q\gg 1$ in the range $T_g\leqslant T\leqslant T_g+6\,\mathrm{K}$ for MTHF does not follow the trend of $Q(T)$ suggested by previous work on OTP. At present, we can only speculate that the feature of Q remaining at high values even at elevated temperatures might correlate with the observation that the stretching exponent β_{KWW} remains constant for MTHF in the present temperature range, instead of increasing with T. Furthermore, OTP and MTHF differ strongly in their glass transitions temperatures, $T_g=246\,\mathrm{K}$ (OTP) vs $T_g=91\,\mathrm{K}$, (MTHF) and in their molecular dipole moments, $\mu=0.07\,\mathrm{D}$ (OTP) vs $\mu=1.38\mathrm{D}$ (MTHF) [28], whereas their fragilities in terms of $F_{1/2}$ are virtually identical [29].

V. SUMMARY AND CONCLUSIONS

The solvation dynamics of a supercooled liquid has been measured near its glass transition in a wide experimental range, $91\,\mathrm{K}\leqslant T\leqslant 97\,\mathrm{K}$ or $T_g\leqslant T\leqslant T_g+6\,\mathrm{K}$ or $3\times 10^{-3}\,\mathrm{s}\leqslant\langle\tau\rangle\leqslant 54\,\mathrm{s}$, by observing the optical $S_0\leftarrow T_1(0\text{-}0)$ transition as a function of time. Analysing both, the average emission energy and the inhomogeneous linewidth, reveals that the orientation correlation decay pattern intrinsic in each relaxing unit is associated with a stretching exponent $\beta_{\mathrm{intr}}=1.00\pm 0.08$, such that the dynamics are observed to be of purely heterogeneous nature. In order to assess the effects of fluctuations in the regime $t\gg\langle\tau\rangle$, we focus on the term $\sqrt{\rho(t)/C(t)}$, which constitutes a sensitive indicator of either true or apparent homogeneity due to rate exchange effects, which would eventually lead to an exponential time dependence regarding the ensemble average. A scrutiny of the corresponding data rules out the possibility that the sites sample the entire τ-space within the experimental time range of up to $t\approx 50\langle\tau\rangle_{\mathrm{KWW}}$. We conclude that the individual time constants remain correlated to their initial values at $t=0$ even at times significantly exceeding $\langle\tau\rangle_{\mathrm{KWW}}$, without claiming that fluctuations are absent.

ACKNOWLEDGMENTS

We thank R. V. Chamberlin for critically reading the manuscript and for many stimulating discussions. Financial support from the Deutsche Forschungsgesellschaft (Ri 545/8-2) is gratefully acknowledged.

[1] M. D. Ediger, C. A. Angell, and S. R. Nagel, J. Phys. Chem. **100**, 13 200 (1996).
[2] K. Schmidt-Rohr and H. W. Spiess, Phys. Rev. Lett. **66**, 3020 (1991).
[3] H. Sillescu, J. Non-Cryst. Solids **243**, 81 (1999).
[4] M. T. Cicerone and M. D. Ediger, J. Chem. Phys. **103**, 5684 (1995).
[5] B. Schiener, R. Böhmer, A. Loidl, and R. V. Chamberlin, Science **274**, 752 (1996).
[6] R. Richert, J. Phys. Chem. B **101**, 6323 (1997).
[7] R. Böhmer, R. V. Chamberlin, G. Diezemann, B. Geil, A. Heuer, G. Hinze, S. C. Kuebler, R. Richert, B. Schiener, H. Sillescu, H. W. Spiess, U. Tracht, and M. Wilhelm, J. Non-Cryst. Solids **235–237**, 1 (1998).
[8] A. Heuer, M. Wilhelm, H. Zimmermann, and H. W. Spiess, Phys. Rev. Lett. **75**, 2851 (1995).
[9] R. Böhmer, G. Diezemann, G. Hinze, and H. Sillescu, J. Chem. Phys. **108**, 890 (1998).
[10] C. Y. Wang and M. D. Ediger, J. Phys. Chem. B **103**, 4177 (1999).
[11] B. Schiener, R. V. Chamberlin, G. Diezemann, and R. Böhmer, J. Phys. Chem. **107**, 7746 (1997).
[12] R. Richert and R. Böhmer, Phys. Rev. Lett. **83**, 4337 (1999).

[13] R. Böhmer, G. Hinze, G. Diezemann, B. Geil, and H. Sillescu, Europhys. Lett. **36**, 55 (1996).
[14] R. Richert, J. Non-Cryst. Solids **235–237**, 41 (1998).
[15] R. Richert and M. Richert, Phys. Rev. E **58**, 779 (1998).
[16] M. Maroncelli, J. MacInnis, and G. R. Fleming, Science **243**, 1674 (1989).
[17] R. Richert, F. Stickel, R. S. Fee, and M. Maroncelli, Chem. Phys. Lett. **229**, 302 (1994).
[18] A. Papazyan and M. Maroncelli, J. Chem. Phys. **102**, 2888 (1995).
[19] R. Richert, J. Phys.: Condens. Matter **8**, 6185 (1996).
[20] R. Richert and A. Wagener, J. Phys. Chem. **95**, 10 115 (1991).
[21] M. L. Horng, J. Gardecki, A. Papazyan, and M. Maroncelli, J. Phys. Chem. **99**, 17311 (1995).
[22] A. Heuer, U. Tracht, S. C. Kuebler, and H. W. Spiess, J. Mol. Struct. **479**, 251 (1999).
[23] N. G. van Kampen, *Stochastic Processes in Physics and Chemistry* (North-Holland, Amsterdam, 1992).
[24] S. C. Kuebler, A. Heuer, and H. W. Spiess, Phys. Rev. E **56**, 741 (1997).
[25] M. T. Cicerone, P. A. Wagner, and M. D. Ediger, J. Phys. Chem. B **101**, 8727 (1997).
[26] M. T. Cicerone and M. D. Ediger, J. Phys. Chem. **97**, 10 489 (1993).
[27] O. Kircher, B. Schiener, and R. Böhmer, Phys. Rev. Lett. **81**, 4520 (1998).
[28] C. Streck and R. Richert, Ber. Bunsenges. Phys. Chem. **98**, 619 (1994).
[29] R. Richert and C. A. Angell, J. Chem. Phys. **108**, 9016 (1998).